OXFORD

*JNCI J Natl Cancer Inst* (2019) 111(3): djy107

doi: 10.1093/jnci/djy107
First published online June 26, 2018
Article

ARTICLE

# The Role of Fibrinogen-Like Protein 2 on Immunosuppression and Malignant Progression in Glioma

Khatri Latha*, Jun Yan*, Yuhui Yang, Loyola V. Gressot, Ling-Yuan Kong, Ganiraju Manyam, Ravesanker Ezhilarasan, Qianghu Wang, Erik P. Sulman, R. Eric Davis, Suyun Huang, Gregory N. Fuller, Arvind Rao, Amy B. Heimberger, Shulin Li, Ganesh Rao*

See the Notes section for the full list of authors' affiliations.
**Correspondence to:** Ganesh Rao, MD, Department of Neurosurgery, Unit 0442, The University of Texas MD Anderson Cancer Center, 1515 Holcombe Blvd., Houston, TX 77030 (e-mail: grao@mdanderson.org); or Shulin Li, PhD, Department of Pediatric Research, Unit 0853, The University of Texas MD Anderson Cancer Center, 1515 Holcombe Blvd., Houston, TX 77030 (e-mail: sli4@mdanderson.org).
*Equal contribution

## Abstract

**Background:** Virtually all low-grade gliomas (LGGs) will progress to high-grade gliomas (HGGs), including glioblastoma, the most common malignant primary brain tumor in adults. A key regulator of immunosuppression, fibrinogen-like protein 2 (FGL2), may play an important role in the malignant transformation of LGG to HGG. We sought to determine the mechanism of FGL2 on tumor progression and to show that inhibiting FGL2 expression had a therapeutic effect.
**Methods:** We analyzed human gliomas that had progressed from low- to high-grade for FGL2 expression. We modeled FGL2 overexpression in an immunocompetent genetically engineered mouse model to determine its effect on tumor progression. Tumors and their associated microenvironments were analyzed for their immune cell infiltration. Mice were treated with an FGL2 antibody to determine a therapeutic effect. Statistical tests were two-sided.
**Results:** We identified increased expression of FGL2 in surgically resected tumors that progressed from low to high grade (n = 10). The Cancer Genome Atlas data showed that LGG cases with overexpression of FGL2 (n = 195) had statistically significantly shorter survival (median = 62.9 months) compared with cases with low expression (n = 325, median = 94.4 months, $P < .001$). In a murine glioma model, HGGs induced with FGL2 exhibited a mesenchymal phenotype and increased $CD4^+$ forkhead box P3 $(FoxP3)^+$ Treg cells, implicating immunosuppression as a mechanism for tumor progression. Macrophages in these tumors were skewed toward the immunosuppressive M2 phenotype. Depletion of Treg cells with anti-FGL2 statistically significantly prolonged survival in mice compared with controls (n = 11 per group, median survival = 90 days vs 62 days, $P = .004$), shifted the phenotype from mesenchymal HGG to proneural LGG, and decreased M2 macrophage skewing.
**Conclusions:** FGL2 facilitates glioma progression from low to high grade. Suppressing FGL2 expression holds therapeutic promise for halting malignant transformation in glioma.

Glioblastoma is the most common malignant primary brain tumor in adults, and despite aggressive treatment, it is incurable (1). Glioblastoma may arise from a more indolent precursor known as low-grade glioma (LGG). Patients with LGG may survive for many years, but after transformation into high-grade glioma (HGG), such as glioblastoma (2), survival rates rapidly decline. As LGGs degenerate to HGGs, they become more immunosuppressive (3,4). HGGs are enriched with immunosuppressive cells such as forkhead box P3 ($FoxP3^+$) T regulatory cells (Tregs), myeloid-derived suppressor cells (MDSCs), and

**Received:** November 3, 2017; **Revised:** April 10, 2018; **Accepted:** May 21, 2018

tumor-associated microglia/macrophages (TAMs) (5–11). An immunosuppressive tumor microenvironment is also associated with the mesenchymal (MES) subtype of glioblastoma, which has a worse prognosis than the less immunosuppressive proneural (PN) subtype (12). We have shown previously that reversing immunosuppression in the stroma prolongs survival in tumor-bearing mice and mitigates tumor progression (3,4,13–15). The mechanisms that underlie immunosuppression, which in turn promotes malignant progression of glioma, are poorly understood.

Fibrinogen-like protein 2 (FGL2), identified by microarray analysis screening as a putative candidate gene modulating Treg function (16), regulates both innate and adaptive immunity (17,18). Cancer cells and interstitial inflammatory cells, including macrophages and endothelial cells, have high FGL2 expression (19–21). Interleukin-2 and interferon-gamma increase human FGL2 mRNA and contribute to hypercoagulability by inducing tumor angiogenesis and metastasis via cytokine induction (22). High levels of FGL2 transcripts have been reported in isolated $CD4^+$ $FoxP3^+$ Tregs (16). Anti-FGL2 antibody can block the activity of $CD8^+CD45RC^{low}$ Tregs (23), indicating that FGL2 is critical to their function. We recently showed that high levels of FGL2 expression in glioblastoma induce immunosuppression by increasing expression of programmed cell death protein 1 (PD-1) and ectonucleoside triphosphate diphosphohydrolase 1. Thus, FGL2 is a hub for glioblastoma-mediated immunosuppression, although its ability to facilitate malignant progression from LGG to HGG is unknown (24).

We hypothesized that FGL2 may cause malignant progression in glioma. We investigated the relationship between cases of malignant progression and survival in patients diagnosed with glioma to FGL2 expression. We analyzed the effect of FGL2 expression in an immunocompetent murine model to determine its ability to cause progression from low- to high-grade glioma. Finally, we evaluated the effect of inhibition of FGL2 expression on malignant progression and survival in tumor-bearing mice.

## Methods

### Expression Analysis

We determined FGL2 mRNA expression levels in tumors from patients with LGG or HGG using The Cancer Genome Atlas data portal (www.cbioportal.org) (25) and the integrated data set of diffuse gliomas (grades II–IV) (26). We identified tumors characterized by the major phenotypes: proneural and mesenchymal (27). We used The Cancer Genome Atlas (TCGA) search terms to categorize patients into two groups: those with FGL2 mRNA expression levels higher than the normalized mean (overexpressors) and those with FGL2 mRNA expression levels lower than the normalized mean (low-expressors).

### Cells and Tissue Samples

GL261 was obtained from the National Cancer Institute. Cells were cultured as described previously (24). Ten pairs of matched LGGs and HGGs from patients whose LGGs underwent malignant transformation were obtained at MD Anderson. The MD Anderson Institutional Review Board approved the study (Protocol No. PA14-0709), and waivers of informed consent and authorization were obtained.

### In Vivo Somatic Cell Transfer in Ntv-a Mice

We used the RCAS/Ntv-a system, a mouse model of platelet-derived growth factor subunit B (PDGFB)–driven gliomas (28). For details, please see the Supplementary Methods (available online). Mice were humanely killed 90 days after injection, or earlier if showing neurological symptoms. The brains were fixed in formalin, embedded in paraffin, and sectioned for immunohistochemical analysis (IHC). Hematoxylin and eosin staining was performed to identify tumors. Experiments were approved by the MD Anderson Institutional Animal Care and Use Committee (Protocol No. 00000900-RN01).

### In Vivo Treatments

Anti-CD25 mAb (250 μg in PBS, PC-6, BioXCell, West Lebanon, NH) was administered intraperitoneally two days per week. Rat IgG (Sigma, St. Louis, MO) was used as control. Anti-FGL2 antibody treatment (Alpha Diagnostic International, San Antonio, Texas) was administered with 250 μg in PBS twice weekly, as previously described (24).

### Determination of Tumor Grade

Tumors were graded by a neuropathologist (GNF), blinded to the vectors injected, using World Health Organization 2016 criteria (29). LGGs were identified by increased cellularity from infiltrating tumor cells. HGGs were identified by microvascular proliferation, or foci of necrosis, or brisk mitotic activity.

The details of the methodology for vector construction, transfection of DF-1 cells, knockout of FGL2 expression in GL261 cells, GL261 mouse model, Ntv-a mouse model, glioma stem cells, immunoblot, enzyme-linked immunosorbent assay, flow cytometry, immunohistochemistry, immunofluorescence, and ethical statements are provided in the Supplementary Methods (available online).

### Statistical Analysis

The incidence of tumors among mouse groups was assessed using the chi-square test. Survival statistics were reported using Kaplan-Meier curves. The log-rank test was used to compare survival curves. The Student *t* test was used to determine differences in antibody expression between injection sets. All statistical tests were two-sided, and a *P* value of less than .05 was considered statistically significant. Statistical analysis was carried out using GraphPad Prism software, version 6 (GraphPad Software, La Jolla, CA). Mutual exclusivity analysis was performed using www.cbioportal.org, and the log odds ratio and Fisher exact test–derived *P* values were reported directly from the portal.

## Results

### The Influence of FGL2 Expression on Survival in LGG and GB

In TCGA patients with glioma (grades II–IV), median survival for FGL2 overexpressors (n = 332) was much shorter (26.3 months) than for low-expressors (n = 332, 88.7 months; log-rank test, $P < .001$) (Figure 1A). In patients with glioblastoma, median survival for FGL2 overexpressors (n = 78) was modestly shorter (12.9 months) than for low-expressors (n = 82, 14.2 months; log-rank

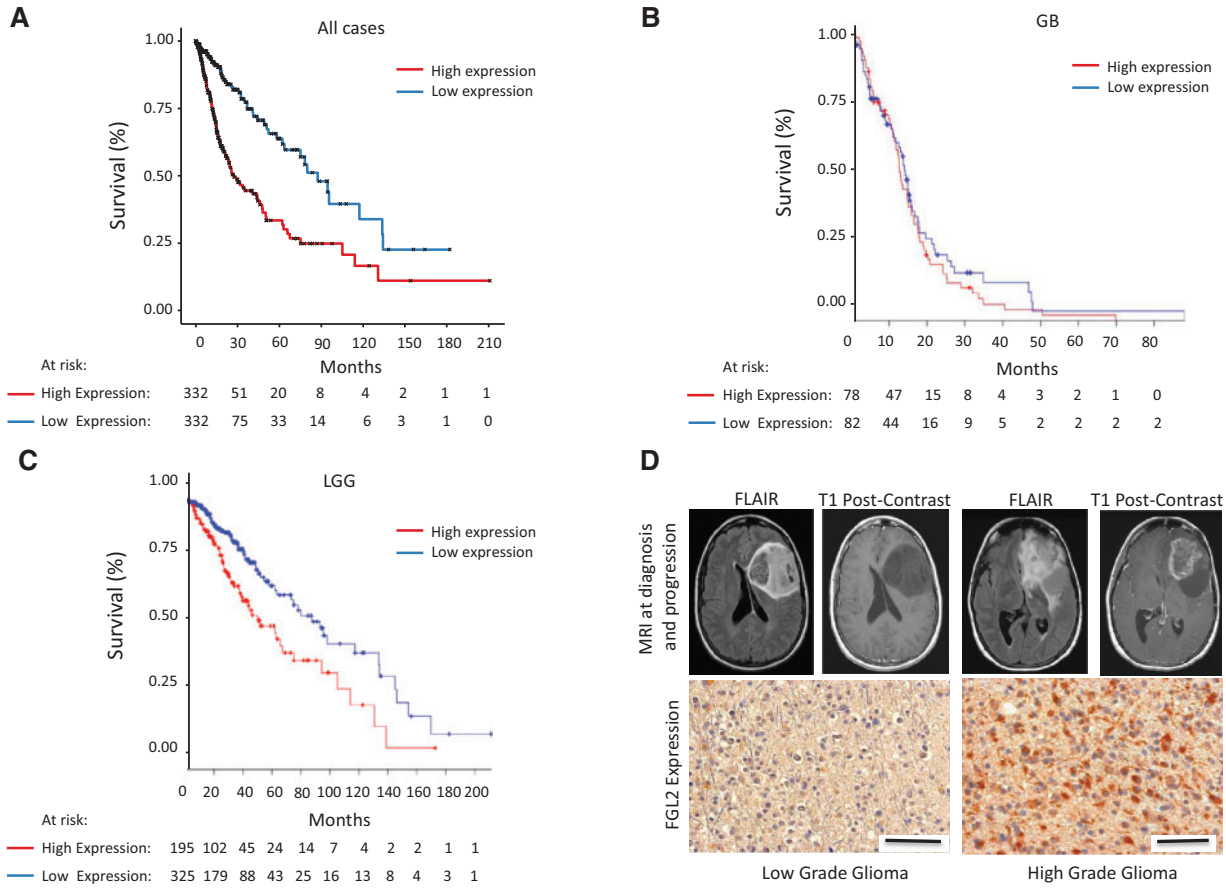


**Figure 1.** The influence of fibrinogen-like protein 2 (FGL2) on survival in low-grade glioma (LGG) and glioblastoma (GB). **A)** Kaplan-Meier curve showing overall survival of The Cancer Genome Atlas (TCGA) glioma (grades II–IV) cases stratified by over- or low-expression of FGL2 mRNA (n = 664, log-rank test, $P < .001$). Median survival in all TCGA patients with LGG or GB stratified by high or low FGL2 expression. **B)** Kaplan-Meier curve showing overall survival of TCGA patients with GB stratified by over- or low-expression of FGL2 mRNA (n = 160, log-rank test, $P = .41$). **C)** Kaplan-Meier curve showing overall survival of TCGA patients with LGG stratified by over- or low-expression of FGL2 (n = 520, log-rank test, $P < .001$). **D)** FGL2 expression in a representative human LGG before and after progression to high-grade glioma (HGG). Representative magnetic resonance images (fluid-attenuated inversion recovery and T1-weighted postcontrast images) at diagnosis and at the time of malignant progression from a patient are shown. The LGG demonstrates a paucity of FGL2 staining, whereas the subsequent HGG in the same patient demonstrates abundant FGL2 staining (magnification, 400×; **scale bar** = 50 $\mu$m). FLAIR = fluid-attenuated inversion recovery; GB = glioblastoma; LGG = low-grade glioma; MRI = magnetic resonance imaging.

ARTICLE

test, $P = .41$) (Figure 1B). However, in patients with LGG, median survival for FGL2 overexpressors (n = 195) was statistically significantly shorter (62.9 months) than for low-expressors (n = 325, 94.4 months; log-rank test, $P < .001$) (Figure 1C). We also analyzed the first and fourth quartiles of FGL2 expression in LGG (n = 224) and found a more profound difference in median survival (log-rank test, $P < .001$) (Supplementary Figure 1, A and B, available online). Although absolute FGL2 expression was higher in patients with glioblastoma than in those with LGG (Supplementary Figure 2A, available online), the survival disadvantage associated with FGL2 expression was substantial for patients with LGG (almost three years). We also analyzed FGL2 expression in the context of molecular characteristics including the statuses of the isocitrate dehydrogenase (IDH) gene (either mutated [MUT] or wild-type [WT]) and the 1p/19q chromosomes (either codeleted [codel] or noncodeleted [noncodel]) (summarized in Supplementary Figures 3–5 and Supplementary Table 1, available online). There was no difference in the distribution of over- and low-expressors in the IDH WT gliomas (Fisher exact test, $P = .05$). There was no statistical difference in overall survival for IDH WT cases between FGL2 over- and low-expressors (log-rank test, $P = .19$). Although there are FGL2 over- and low-expressors in both IDH MUT and WT subtypes in LGG, there was a statistically significantly higher number of FGL2 overexpressors in the IDH WT group compared with FGL2 low-expressors (Fisher exact test, $P < .001$). In all gliomas, we did find a statistical difference in the IDH MUT cases with respect to overall survival between the over- and low-expressors (log-rank test, $P = .008$). In IDH MUT LGGs, we found a statistically significant difference in survival between FGL2 over- and low-expressors (log-rank test, $P = .01$) but not in IDH WT LGGs (log-rank test, $P = .24$). In both the codel and noncodel glioma cases, there are over- and low-expressors represented, although we found a statistically significantly higher number of FGL2 overexpressors in the noncodel group compared with the codel group (Fisher exact test, $P < .001$). All IDH MUT codel cases are from the LGG cohort, and there was no difference in overall survival in over- and low-expressors of FGL2 (log-rank test, $P = .20$). Similarly, we did not find a statistical difference in survival in the noncodel LGG cases between the over- and low-expressors of FGL2 (log-rank test, $P = .12$). From these results, we observe FGL2 overexpression in IDH MUT and WT, codel and noncodel gliomas, although poorer survival is associated with IDH MUT cases. As the majority of secondary high-grade gliomas evolve from IDH

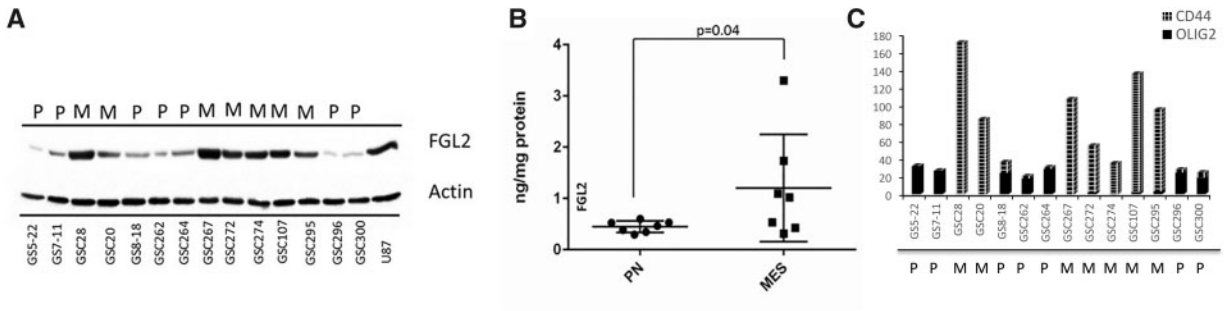


**Figure 2.** Fibrinogen-like protein 2 (FGL2) expression in glioblastoma stem cells and in human tumors. **A)** Immunoblot analysis of FGL2 expression in proneural (PN/P) and mesenchymal (MES/M) glioma stem cells (GSCs). Actin was used as the loading control. U87 was used as the positive control for FGL2 expression. **B)** Confirmation of FGL2 expression in GSCs using enzyme-linked immunosorbent assay (*t* test, two-sided, $P = .04$). **Error bars** = SD. **C)** Characterization of GSC lines for PN and MES signatures using RNA sequencing for Olig2 and CD44 markers. FGL2 = fibrinogen-like protein 2; MES/M = mesenchymal; PN/P = proneural.

MUT low-grade gliomas, these results suggest a role for FGL2 expression in malignant transformation.

We tested the expression of FGL2 in a panel of human LGGs (n = 10) that transformed into HGG (Figure 1D; Supplementary Table 2, available online). We found that eight of 10 HGGs had statistically significantly higher FGL2 expression than their LGG precursors ($P = .02$) (Supplementary Figure 2B, available online), suggesting that malignant transformation may have been associated with FGL2 upregulation during the disease course. Taken together, these results suggest that FGL2 plays a role in promoting malignant progression to HGG.

## Expression Level of FGL2 and Glioblastoma Subtypes

Glioblastoma is heterogeneous, including proneural and mesenchymal GSCs, with distinct subtypes that exist on a continuum (30). GSCs recapitulate the genomic landscape of GBMs (27,31). Like HGGs with a mesenchymal signature, mesenchymal GSCs display an aggressive phenotype in vitro and in vivo (32). TCGA glioblastoma data demonstrated higher FGL2 expression in patients with the mesenchymal subtype (46 of 56, 82.1%) than in those with the proneural subtype (17 of 56, 30.4%) (data not shown).

We compared GSC lines and observed statistically significantly higher FGL2 expression in mesenchymal GSCs than in proneural GSCs (Figure 2A). We used enzyme-linked immunosorbent assay to validate FGL2 expression levels in the proneural (0.45 ±0.04 ng/mg protein) and mesenchymal (1.2 ± 0.3 ng/mg protein) GSCs (Figure 2B) and confirmed statistically significantly higher FGL2 expression in the mesenchymal GSCs (*t* test, $P = .04$). GSCs were characterized for subtype using RNA sequencing for CD44, FN1, CHI3L1, and CTGF for the mesenchymal subtype markers and Olig2, SOX2, SOX9, and PROM1 for the proneural subtype markers (Figure 2C; Supplementary Figure 6, available online). These results from the TCGA and GSC cell lines suggest that the mesenchymal subtype of high-grade glioma correlates with increased FGL2 expression.

## The Effect of FGL2 Overexpression on Malignant Progression in Vivo

We expressed FGL2 in Ntv-a mice to evaluate the capacity of FGL2 to drive malignant tumor progression. The RCAS/Ntv-a model is suited to study malignant progression in glioma because endogenous tumors form from glioneuronal precursor cells in immunocompetent mice (33). Expression of the PDGFB ligand alone in Ntv-a mice induces predominantly low-grade tumors recapitulating human LGG. We overexpressed PDGFB alone, FGL2 alone, or both in Ntv-a mice. FGL2 expression was verified (Supplementary Figure 7, available online). None of the mice in the RCAS-FGL2 group developed tumors. In the RCAS-PDGFB+FGL2 group, median survival was 63 days, statistically significantly shorter than in the RCAS-PDGFB group (90 days; log-rank test, $P = .003$) (Figure 3A). Tumor formation rates and grades for each group were compared (Supplementary Tables 3 and 4, available online). In the RCAS-PDGFB group, 31 of 32 mice formed tumors (97.0%). Of these, 22 were low grade (71.0%) and nine were high grade (29.0%). In the RCAS-PDGFB+FGL2 group, 33 of 37 mice formed tumors (89.1%): nine were low grade (27.3%) and 24 were high grade (73.0%). The RCAS-PDGFB+FGL2 group had statistically significantly more high-grade tumors than the RCAS-PDGFB group (chi-square test, $P < .001$) (data not shown).

Gliomas, regardless of grade, induced by RCAS-PDGFB+FGL2 had statistically significantly increased CD44 staining compared with RCAS-PDGFB (*t* test, $P < .001$) (Figure 3B), which is consistent with the mesenchymal subtype. In contrast, gliomas, regardless of grade, induced by RCAS-PDGFB showed statistically significantly higher expression of Olig2, consistent with the proneural subtype compared with RCAS-PDGFB+FGL2 (*t* test, $P < .001$) (Figure 3C). We analyzed the relationship between the expression of FGL2/CD44 and FGL2/OLIG2 in TCGA LGG cases. FGL2 expression statistically significantly cooccurred with CD44 (log OR = 1.95; Fisher exact test $P < .001$) and demonstrated mutual exclusivity with Olig2 (log OR < –3; Fisher exact test, $P = .28$). Thus, co-expression of FGL2 with PDGFB in Ntv-a mice induces high-grade gliomas with a mesenchymal phenotype.

## The Effect of FGL2 Depletion on Glioma Formation in GL261 Intracranial Tumors

To confirm the role of FGL2 in glioma formation and progression, we knocked out FGL2 in GL261 cells. The mRNA expression level of FGL2 was decreased in sorted green fluorescent protein–positive GL261-FGL2KO cells compared with GL261 parent cells (Figure 4A). None of the eight C57/BL6 mice inoculated intracranially with GL261-FGL2KO cells developed tumors, whereas eight of eight mice injected with GL261 cells developed tumors (Figure 4B). These results suggest that FGL2 expression is required for GL261 cells to form aggressive tumors in mice.

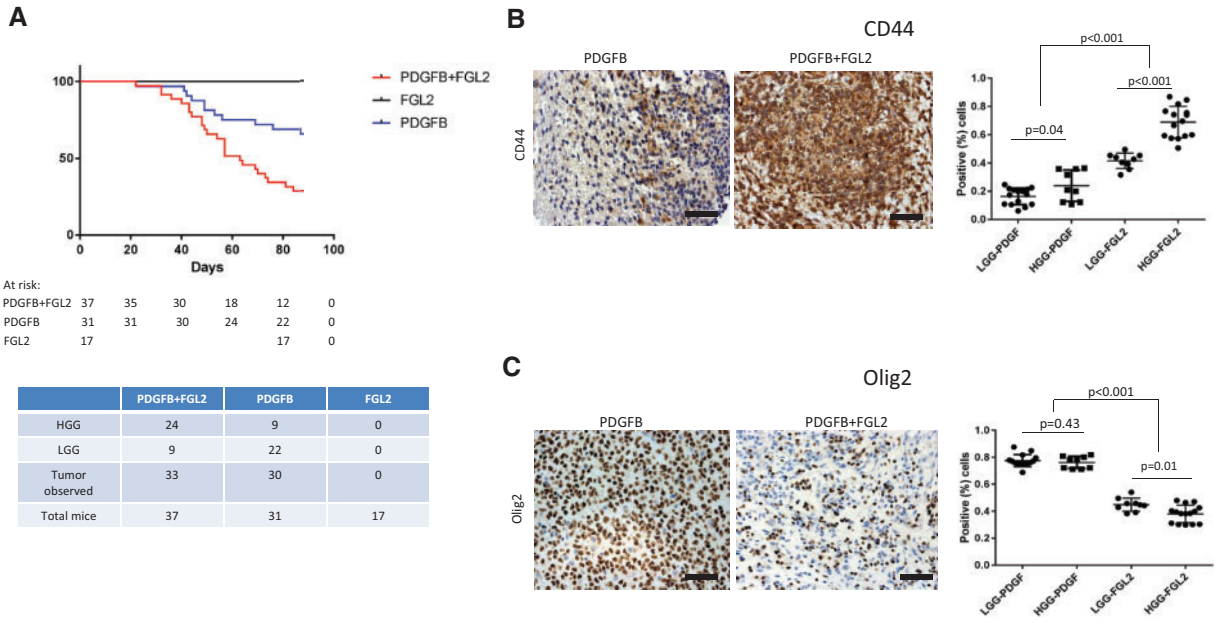


| | PDGFB+FGL2 | PDGFB | FGL2 |
|---|---|---|---|
| HGG | 24 | 9 | 0 |
| LGG | 9 | 22 | 0 |
| Tumor observed | 33 | 30 | 0 |
| Total mice | 37 | 31 | 17 |

**Figure 3.** The effect of fibrinogen-like protein 2 (FGL2) overexpression on malignant progression in vivo. **A)** Kaplan-Meier analysis demonstrating symptom-free survival in Ntv-a mice from the replication-competent ASLV long terminal repeat with a splice (RCAS) platelet-derived growth factor subunit B (PDGFB), RCAS-PDGFB+FGL2, or RCAS-FGL2 groups. **B and C)** CD44 and Olig2 expression in RCAS-PDGFB and RCAS-PDGFB+FGL2 LGGs and HGGs. Immunohistochemical staining of representative tumor sections (magnification, 400×; **scale bar** = 50 $\mu$m). **Left)** Scatter plot demonstrating differences in CD44 and Olig2 expression between the two groups (*t* test, two-sided). FGL2 = fibrinogen-like protein 2; HGG = high-grade glioma; LGG = low-grade glioma; PDGF = platelet-derived growth factor; PDGFB = platelet-derived growth factor subunit B.

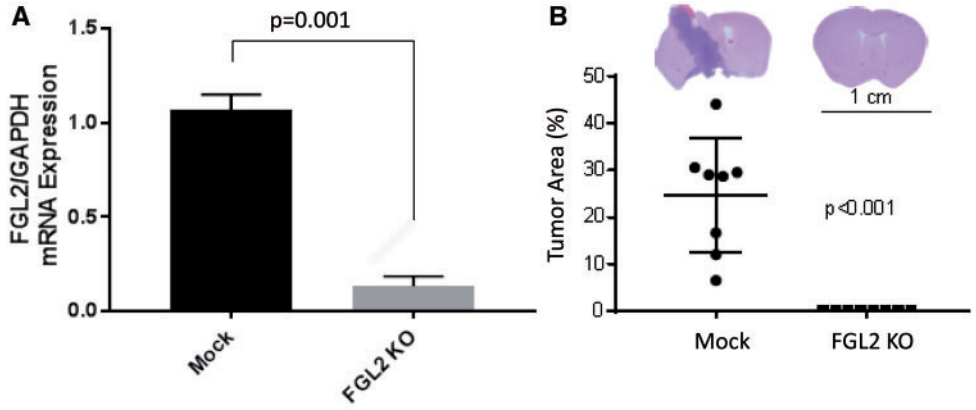


**Figure 4.** The effect of fibrinogen-like protein 2 (FGL2) depletion on glioma formation in GL261 intracranial tumors. **A)** FGL2 mRNA expression in mock and FGL2-KO GL261 cells. Glyceraldehyde 3-phosphate dehydrogenase was used for normalization. **B)** Whole-mount photograph showing tumor occurrence in GL261-FGL2-knockout (GL261-FGL2KO) mice and the mock GL261 mice. FGL2 = fibrinogen-like protein 2; KO = knockout.

## The Influence of FGL2 Expression on the Recruitment of Immune Cells to the Tumor Microenvironment

Previously, we showed that FGL2 augments glioma immunosuppression by increasing the expression levels of PD-1 and CD39 in $CD45^+$ leukocytes (24). FGL2 acts as a Treg effector by suppressing T-cell activities in a FoxP3-dependent manner (16). We investigated the expression of FoxP3 in FGL2-expressing tumors to determine the mechanism by which FGL2 facilitates the transformation of PDGFB-induced LGG to HGG. FoxP3 staining was statistically significantly higher in the RCAS-PDGFB+FGL2 group than in the RCAS-PDGFB group (*t* test, $P < .001$) (Figure 5A; Supplementary Figure 8A, available online). TCGA analysis also showed a statistically significant co-occurrence of FGL2 and FoxP3 mRNA in glioblastoma (log OR = 1.62; Fisher exact test, $P < .001$) (Supplementary Figure 8B, available online). In LGGs, FGL2 and FoxP3 also demonstrate statistically significant co-occurrence (log OR = 2.91; Fisher exact test, $P < .001$).

We performed fluorescence-activated cell sorting (FACS) analysis of Tregs ($CD4^+FoxP3^+$) in both the RCAS-PDGFB+FGL2 and RCAS-PDGFB groups at different time points (Figure 5B). Tregs are known to populate the microenvironment of HGGs to a greater degree than LGGs (34). The RCAS-PDGFB+FGL2 tumors had statistically significantly more immunosuppressive $CD4^+FoxP3^+$ cells than the RCAS-PDGFB tumors from as early as day 20 in Ntva mice (*t* test, $P = .05$). To show that blocking Tregs could have a therapeutic effect (supporting the inhibition of

ARTICLE

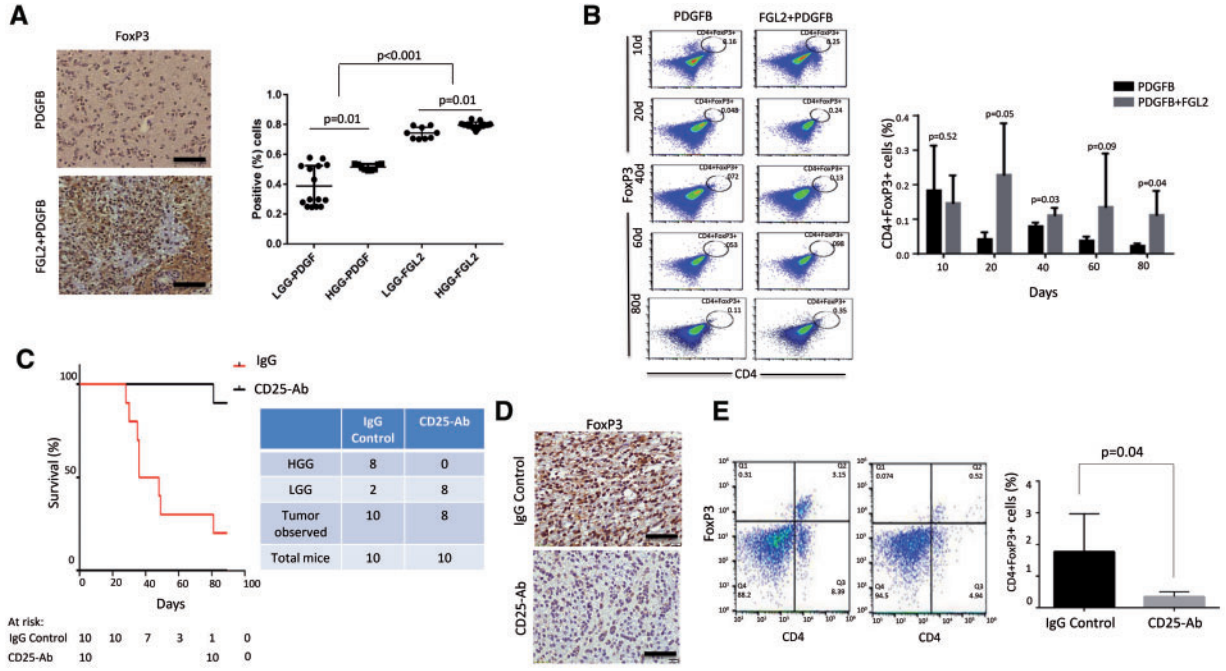


**Figure 5.** The influence of fibrinogen-like protein 2 (FGL2) expression on the recruitment of immune cells to the tumor microenvironment. **A)** Forkhead box P3 (FoxP3) expression in replication-competent ASLV long terminal repeat with a splice (RCAS) platelet-derived growth factor subunit B (PDGFB) and RCAS-PDGFB+FGL2 tumors. Scatter plot demonstrating the difference in FoxP3 expression between the two groups (magnification, 400×; **scale bar** = 50 $\mu$m) among LGGs and HGGs from each injection set. **B)** Immunosuppressive $CD4^+FoxP3^+$ cells in the tumor microenvironment were analyzed by fluorescence-activated cell sorting at different time points (10, 20, 40, 60, and 80 days). Data are presented as the mean ± standard deviation (n = 5 mice). An unpaired *t* test was used to calculate the two-sided *P* values. **C)** Kaplan-Meier curve demonstrating symptom-free survival in Ntv-a mice injected with replication-competent ASLV long terminal repeat with a splice (RCAS) platelet-derived growth factor subunit B (PDGFB)+FGL2 and treated with anti-CD25 antibody or rat immunoglobulin G (IgG) control starting three weeks after inoculation (n = 10 mice). **D)** Immunohistochemical staining of FoxP3 expression between treated and control groups (magnification, 400×; **scale bar** = 50 $\mu$m). **E)** Flow analysis of the depletion of $CD4^+FoxP3^+$ cells in the CD25 antibody–treated tumor compared with IgG control tumors (n = 5 mice). An unpaired *t* test was used to calculate the two-sided *P* values. FGL2 = fibrinogen-like protein 2; HGG = high-grade glioma; LGG = low-grade glioma; PDGF = platelet-derived growth factor; PDGFB = platelet-derived growth factor subunit B.

FGL2 as a therapeutic strategy), we administered CD25 antibody to Ntv-a mice injected with RCAS-PDGFB+FGL2 (35). Mice treated with CD25 (n = 10) had a statistically significantly longer survival than mice treated with IgG (n = 10, log-rank test, $P < .001$) (Figure 5C). The incidence of HGGs was also statistically significantly lower in the CD25 antibody–treated mice compared with IgG controls. We confirmed the reduction of FoxP3 Tregs in these CD25 antibody–treated mice both by IHC and FACS analysis compared with IgG control–treated mice (Figure 5, D and E).

Results from the glioblastoma TCGA data analysis shows that FGL2 expression statistically significantly co-occurs with immunosuppressive macrophage markers including Iba1 (log OR = 1.3; Fisher exact test, $P < .001$), CD11b/c (log OR = 1.63; Fisher exact test, $P < .001$), and CD68 (log OR = 2.01; Fisher exact test, $P < .001$). To validate TCGA findings, we immunostained the RCAS-FGL2 and RCAS-PDGFB+FGL2 tumors to determine the expression of macrophage markers. We observed an increase in expression of microglial markers in RCAS-PDGFB+FGL2 tumors compared with RCAS-PDGFB tumors (Supplementary Figure 9A, available online). M2 polarization of FGL2-induced macrophages was validated by costaining for Iba1 and Arginase 1 in the RCAS-PDGFB+FGL2 and RCAS-PDGFB tumors. RCAS-PDGFB+FGL2 tumors had statistically significantly higher expression of Arginase $1^+$/$Iba1^+$ macrophages than RCAS-PDGFB tumors (Supplementary Figure 9B, available online). These data suggest that FGL2-mediated immune suppression includes the accumulation of M2 polarized macrophages in the tumor microenvironment.

## The Effect of FGL2 Inhibition on Overall Survival, Macrophage Polarization, and Treg Infiltration

To validate the immune-suppressive mechanism of FGL2 in the tumor microenvironment, extracellular or soluble FGL2 expression was blocked using anti-FGL2 antibody. Ntv-a mice injected with RCAS-PDGFB+FGL2 were treated with anti-FGL2 antibody (24) or IgG control. Tumor progression and immune suppressors were investigated in treated and control mice beginning three weeks after inoculation. Anti-FGL2 antibody–treated mice (n = 11) had statistically significantly longer median symptom-free survival (90 days) than control mice (n = 11, 62 days; log-rank test, $P = .004$) (Figure 6A).

Associated with increased survival time by anti-FGL2 antibody treatment, the expression of CD44 was statistically significantly lower in the anti-FGL2 antibody–treated tumors than in the IgG-treated tumors, whereas Olig2 expression was statistically significantly higher than control tumors (Figure 6B), indicating maintenance of the proneural subtype in the anti-FGL2 antibody–treated tumors (Supplementary Figure 10, available online).

Because we found more Tregs in the tumors from the RCAS-PDGFB+FGL2 group than from the RCAS-PDGFB group, we investigated whether blocking FGL2 could reduce the number of Tregs early in the disease course. We treated mice with tumors induced by RCAS-PDGFB+FGL2 with anti-FGL2 antibody and quantified $CD4^+FoxP3^+$ Tregs at 20 days after treatment. The anti-FGL2 antibody–treated mice had fewer Tregs at 20 days

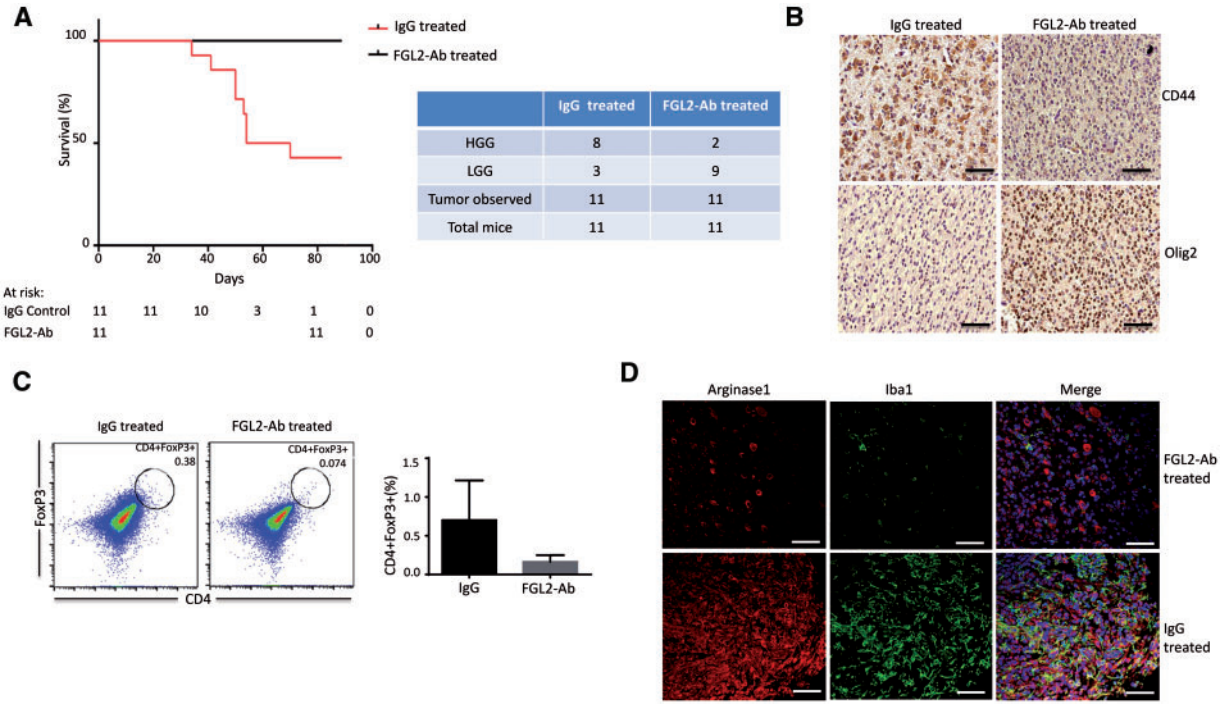


| | IgG treated | FGL2-Ab treated |
|---|---|---|
| HGG | 8 | 2 |
| LGG | 3 | 9 |
| Tumor observed | 11 | 11 |
| Total mice | 11 | 11 |

**Figure 6.** The effect of fibrinogen-like protein 2 (FGL2) inhibition on overall survival, macrophage polarization, and Treg infiltration. **A)** Kaplan-Meier curve demonstrating symptom-free survival in Ntv-a mice injected with replication-competent ASLV long terminal repeat with a splice (RCAS) platelet-derived growth factor subunit B (PDGFB)+FGL2 and treated with anti-FGL2 antibody (FGL2-Ab) or immunoglobulin G (IgG) control starting three weeks after inoculation (n = 11 mice). **B)** CD44 and Olig2 expression in representative IgG control– and FGL2-Ab–treated tumors (magnification, 400×; **scale bar** = 50 $\mu$m). **C)** Immunosuppressive CD4$^+$forkhead box P3 (FoxP3)$^+$ cells in the tumor microenvironment were analyzed by fluorescence-activated cell sorting after 20 days of treatment with anti-FGL2 antibody or IgG antibody (control). Data are presented as the mean ± standard deviation (n = 4 mice). An unpaired *t* test was used to calculate the two-sided *P* values. **D)** Expression of Arginase 1$^+$/Iba1$^+$ cells in the RCAS-PDGFB+FGL2 tumors treated with IgG or anti-FGL2 antibody. Representative immunofluorescence staining for Arginase 1 (**red**) and Iba1 (**green**) macrophages (magnification, 400×; **scale bar** = 50 $\mu$m). FGL2 = fibrinogen-like protein 2; HGG = high-grade glioma; LGG = low-grade glioma.

than the IgG-treated mice, although the difference was not statistically significant ($P = .08$) (Figure 6C). This result shows that anti-FGL2 antibody treatment may successfully mitigate immunosuppression in the tumor microenvironment. The anti-FGL2 antibody–treated tumors also had fewer Arginase 1$^+$/Iba1$^+$ macrophages (Figure 6D), demonstrating suppressed M2 polarization and decreased Treg accumulation.

## Discussion

The response to immunotherapy in glioblastoma is undermined by immunosuppressive effectors including FoxP3$^+$ regulatory T cells, M2 macrophages, immunosuppressive cytokines, immune checkpoints, MDSCs, and TAMs. FGL2 acts as a Treg effector in a FoxP3-dependent manner (16,36) and regulates immunity (37). FGL2 has been associated with suppression of Th1-polarized immune responses in several models (17,38,39). Although our results show that FGL2 is sufficient to promote the transformation of LGGs into HGGs by regulating the tumor immune environment, others have shown different roles of FGL2 in supporting tumor growth. FGL2 stimulates hepatocellular and prostate tumor cell growth by facilitating angiogenesis via its prothrombin effect (21,40). In colorectal cancer, FGL2 has been shown to promote progression and metastasis by inducing epithelial-to-mesenchymal transition in tumor cells (41). Contrary to these mechanisms, we showed previously in an HGG model that FGL2 promotes tumor cell growth through the induction of immune suppression (24). Here, we investigated FGL2 expression as a mechanism for malignant progression in glioma. LGG progression to HGG is known to be associated with immunosuppression (34,42–44). We show that FGL2 is a key regulator of transformation of LGG to HGG by inducing a tumor microenvironment enriched with Tregs and M2-polarized macrophages. Higher expression of FGL2 in LGG results in poor survival. FGL2 expression promoted malignant progression by inducing HGGs consistent with the immunosuppressive mesenchymal phenotype and facilitated the accumulation of intratumoral Tregs and M2-polarized macrophages (45). Blocking Tregs or FGL2 expression in these tumors prolonged survival time and reduced immune-suppressive cells. The FGL2-Ab-treated tumors were consistent with proneural glioblastoma, whereas the IgG-treated mice retained immunosuppressive and mesenchymal features, demonstrating the fungible nature of the glioma phenotypes (45).

Tumors did not form in the mice after inoculation with the FGL2 knockout GL261 cells in the present study. In Ntv-a mice, blocking FGL2 via its cognate antibody prolonged survival, although we did observe tumors in these treated mice, which is due to the potent effect of PDGFB and FGL2 on inducing gliomas. We found that FGL2 expressed in CD4$^+$FoxP3$^+$ Treg cells is critical for the development of immunosuppression in these mice to facilitate malignant progression.

There are limitations to our study. We relied on transcription profiling, and there are biases inherent to this technique. However, we did validate protein expression of FGL2 in a small sample of tumors that had progressed from low to high grade. The heterogeneous nature of gliomas makes it difficult to generalize the possible therapeutic effect of FGL2 inhibition in

patients. Although the survival advantage after treatment is robust in mice, it may not be in patients who have been previously treated and are on immunosuppressive glucocorticoids. Further, gliomas are notorious for circumventing the inhibition of a single pathway or signaling molecule. Finally, the indolent nature of LGGs means that the timing of treatment may be challenging. However, it may be possible to initiate treatment when radiographic changes occur, which often herald the transformation from low- to high-grade glioma.

Several studies have targeted FGL2 as a potential therapy. Liu et al. (46) identified peptides that block the biological activity of FGL2 in vitro. However, none yielded any benefit in blocking tumor progression in vivo (S. Li, PhD. Unpublished Data, 2016). Notably, antimouse FGL2 monoclonal antibody protects mice from lethal infective diseases, such as viral hepatitis (47), but this antibody has not been studied in tumor models. In the current study, treatment with anti-FGL2 antibody reduced the levels of immunosuppressive $CD4^{+}FoxP3^{+}$ cells and mitigated the M2 skew. These findings support targeting the FGL2 pathway to delay or prevent malignant progression in glioma. Other approaches for targeting FGL2 may include small molecule inhibitors of STAT1, C/EBP$\alpha$, and HNF4 to suppress FGL2 induction in tumor cells (48–50). Suppressing FGL2 expression in tumor cells or within the tumor microenvironment holds therapeutic promise for cancer immunotherapy in glioblastoma.

## Funding

This work was supported by the National Institutes of Health (grant numbers K08NS070928 and R01NS094615 to GR and R01CA20349301A1 to SL) and the National Cancer Institute SPORE in Brain Cancer (P50 CA127001) and the SPORE Career Development Program (P50 CA127001-07 to KL), the Marnie Rose Foundation (GR), and The Broach Foundation for Brain Cancer Research. This work was also supported by MD Anderson Cancer Center Core Grant NCI CA016672, including the DNA Analysis Facility, the Sequencing and Microarray Facility, and the Monoclonal Antibody Facility.

## Notes

Affiliations of authors: Departments of Neurosurgery (KL, YY, LVG, LYK, ABH, SH, GR), Pediatric Research (JY, SL), Bioinformatics and Computational Biology (GM, QW, AR), Radiation Oncology (RE, EPS), Lymphoma and Myeloma (RED), and Pathology (GNF), The University of Texas MD Anderson Cancer Center, Houston, TX.

The funders had no role in the design of the study; the collection, analysis, or interpretation of the data; the writing of the manuscript; or the decision to submit the manuscript for publication.

The authors have no conflicts of interest to disclose.

## References

1. Stupp R, Hegi ME, Mason WP, et al. Effects of radiotherapy with concomitant and adjuvant temozolomide versus radiotherapy alone on survival in glioblastoma in a randomised phase III study: 5-year analysis of the EORTC-NCIC trial. *Lancet Oncol*. 2009;10(5):459–466.
2. Huse JT, Phillips HS, Brennan CW. Molecular subclassification of diffuse gliomas: Seeing order in the chaos. *Glia*. 2011;59(8):1190–1199.
3. Kong LY, Wu AS, Doucette T, et al. Intratumoral mediated immunosuppression is prognostic in genetically engineered murine models of glioma and correlates to immunotherapeutic responses. *Clin Cancer Res*. 2010;16(23):5722–5733.
4. Doucette TA, Kong LY, Yang Y, et al. Signal transducer and activator of transcription 3 promotes angiogenesis and drives malignant progression in glioma. *Neuro Oncol*. 2012;14(9):1136–1145.
5. Gajewski TF, Schreiber H, Fu YX. Innate and adaptive immune cells in the tumor microenvironment. *Nat Immunol*. 2013;14(10):1014–1022.
6. Khaled YS, Ammori BJ, Elkord E. Myeloid-derived suppressor cells in cancer: Recent progress and prospects. *Immunol Cell Biol*. 2013;91(8):493–502.
7. Mantovani A, Romero P, Palucka AK, et al. Tumour immunity: Effector response to tumour and role of the microenvironment. *Lancet*. 2008;371(9614):771–783.
8. Sarkar S, Doring A, Zemp FJ, et al. Therapeutic activation of macrophages and microglia to suppress brain tumor-initiating cells. *Nat Neurosci*. 2014;17(1):46–55.
9. Nduom EK, Weller M, Heimberger AB. Immunosuppressive mechanisms in glioblastoma. *Neuro Oncol*. 2015;17(suppl 7):vii9–vii14.
10. Razavi SM, Lee KE, Jin BE, et al. Immune evasion strategies of glioblastoma. *Front Surg*. 2016;3:11.
11. Perng P, Lim M. Immunosuppressive mechanisms of malignant gliomas: Parallels at non-CNS sites. *Front Oncol*. 2015;5:153.
12. Doucette T, Rao G, Rao A, et al. Immune heterogeneity of glioblastoma subtypes: Extrapolation from the cancer genome atlas. *Cancer Immunol Res*. 2013;1(2):112–122.
13. Wei J, Wang F, Kong LY, et al. miR-124 inhibits STAT3 signaling to enhance T cell-mediated immune clearance of glioma. *Cancer Res*. 2013;73(13):3913–3926.
14. Xu S, Wei J, Wang F, et al. Effect of miR-142-3p on the M2 macrophage and therapeutic efficacy against murine glioblastoma. *J Natl Cancer Inst*. 2014;106(8):dju162.
15. Schrand B, Berezhnoy A, Brenneman R, et al. Targeting 4-1BB costimulation to the tumor stroma with bispecific aptamer conjugates enhances the therapeutic index of tumor immunotherapy. *Cancer Immunol Res*. 2014;2(9):867–877.
16. Zheng Y, Josefowicz SZ, Kas A, et al. Genome-wide analysis of Foxp3 target genes in developing and mature regulatory T cells. *Nature*. 2007;445(7130):936–940.
17. Shalev I, Wong KM, Foerster K, et al. The novel CD4+CD25+ regulatory T cell effector molecule fibrinogen-like protein 2 contributes to the outcome of murine fulminant viral hepatitis. *Hepatology*. 2009;49(2):387–397.
18. Hu J, Yan J, Rao G, et al. The duality of Fgl2 - secreted immune checkpoint regulator versus membrane-associated procoagulant: Therapeutic potential and implications. *Int Rev Immunol*. 2016;35(4):325–339.
19. Ding JW, Ning Q, Liu MF, et al. Fulminant hepatic failure in murine hepatitis virus strain 3 infection: Tissue-specific expression of a novel fgl2 prothrombinase. *J Virol*. 1997;71(12):9223–9230.
20. Su K, Chen F, Yan WM, et al. Fibrinogen-like protein 2/fibroleukin prothrombinase contributes to tumor hypercoagulability via IL-2 and IFN-gamma. *World J Gastroenterol*. 2008;14(39):5980–5989.
21. Liu Y, Xu L, Zeng Q, et al. Downregulation of FGL2/prothrombinase delays HCCLM6 xenograft tumour growth and decreases tumour angiogenesis. *Liver Int*. 2012;32(10):1585–1595.
22. Fontenot JD, Rasmussen JP, Gavin MA, et al. A function for interleukin 2 in Foxp3-expressing regulatory T cells. *Nat Immunol*. 2005;6(11):1142–1151.
23. Guillonneau C, Hill M, Hubert FX, et al. CD40Ig treatment results in allograft acceptance mediated by CD8CD45RC T cells, IFN-gamma, and indoleamine 2,3-dioxygenase. *J Clin Invest*. 2007;117(4):1096–1106.
24. Yan J, Kong LY, Hu J, et al. FGL2 as a Multimodality regulator of tumor-mediated immune suppression and therapeutic target in gliomas. *J Natl Cancer Inst*. 2015;107(8):djv137.
25. Cerami E, Gao J, Dogrusoz U, et al. The cBio cancer genomics portal: An open platform for exploring multidimensional cancer genomics data. *Cancer Discov*. 2012;2(5):401–404.
26. Ceccarelli M, Barthel FP, Malta TM, et al. Molecular profiling reveals biologically discrete subsets and pathways of progression in diffuse glioma. *Cell*. 2016;164(3):550–563.
27. Verhaak RG, Hoadley KA, Purdom E, et al. Integrated genomic analysis identifies clinically relevant subtypes of glioblastoma characterized by abnormalities in PDGFRA, IDH1, EGFR, and NF1. *Cancer Cell*. 2010;17(1):98–110.
28. Holland EC, Varmus HE. Basic fibroblast growth factor induces cell migration and proliferation after glia-specific gene transfer in mice. *Proc Natl Acad Sci U S A*. 1998;95(3):1218–1223.
29. Louis DN, Perry A, Reifenberger G, et al. The 2016 World Health Organization Classification of tumors of the central nervous system: A summary. *Acta Neuropathol*. 2016;131(6):803–820.
30. Nakano I. Stem cell signature in glioblastoma: Therapeutic development for a moving target. *J Neurosurg*. 2015;122(2):324–330.
31. Wang Q, Hu B, Hu X, et al. Tumor evolution of glioma-intrinsic gene expression subtypes associates with immunological changes in the microenvironment. *Cancer Cell*. 2018;33(1):152.
32. Bhat KP, Balasubramaniyan V, Vaillant B, et al. Mesenchymal differentiation mediated by NF-kappaB promotes radiation resistance in glioblastoma. *Cancer Cell*. 2013;24(3):331–346.

33. Holland EC, Celestino J, Dai C, et al. Combined activation of Ras and Akt in neural progenitors induces glioblastoma formation in mice. *Nat Genet*. 2000; 25(1):55–57.
34. Heimberger AB, Abou-Ghazal M, Reina-Ortiz C, et al. Incidence and prognostic impact of FoxP3+ regulatory T cells in human gliomas. *Clin Cancer Res*. 2008;14(16):5166–5172.
35. Grauer OM, Nierkens S, Bennink E, et al. CD4+FoxP3+ regulatory T cells gradually accumulate in gliomas during tumor growth and efficiently suppress antiglioma immune responses in vivo. *Int J Cancer*. 2007;121(1):95–105.
36. Williams LM, Rudensky AY. Maintenance of the Foxp3-dependent developmental program in mature regulatory T cells requires continued expression of Foxp3. *Nat Immunol*. 2007;8(3):277–284.
37. Chan CW, Kay LS, Khadaroo RG, et al. Soluble fibrinogen-like protein 2/fibroleukin exhibits immunosuppressive properties: Suppressing T cell proliferation and inhibiting maturation of bone marrow-derived dendritic cells. *J Immunol*. 2003;170(8):4036–4044.
38. Khattar R, Luft O, Yavorska N, et al. Targeted deletion of FGL2 leads to increased early viral replication and enhanced adaptive immunity in a murine model of acute viral hepatitis caused by LCMV WE. *PLoS One*. 2013;8(10): e72309.
39. Joller N, Lozano E, Burkett PR, et al. Treg cells expressing the coinhibitory molecule TIGIT selectively inhibit proinflammatory Th1 and Th17 cell responses. *Immunity*. 2014;40(4):569–581.
40. Rabizadeh E, Cherny I, Lederfein D, et al. The cell-membrane prothrombinase, fibrinogen-like protein 2, promotes angiogenesis and tumor development. *Thromb Res*. 2015;136(1):118–124.
41. Qin WZ, Li QL, Chen WF, et al. Overexpression of fibrinogen-like protein 2 induces epithelial-to-mesenchymal transition and promotes tumor progression in colorectal carcinoma. *Med Oncol*. 2014;31(9):181.
42. Bingle L, Brown NJ, Lewis CE. The role of tumour-associated macrophages in tumour progression: Implications for new anticancer therapies. *J Pathol*. 2002; 196(3):254–265.
43. Komohara Y, Ohnishi K, Kuratsu J, et al. Possible involvement of the M2 anti-inflammatory macrophage phenotype in growth of human gliomas. *J Pathol*. 2008;216(1):15–24.
44. Solinas G, Germano G, Mantovani A, et al. Tumor-associated macrophages (TAM) as major players of the cancer-related inflammation. *J Leukoc Biol*. 2009;86(5):1065–1073.
45. Phillips HS, Kharbanda S, Chen R, et al. Molecular subclasses of high-grade glioma predict prognosis, delineate a pattern of disease progression, and resemble stages in neurogenesis. *Cancer Cell*. 2006;9(3):157–173.
46. Liu H, Yang PS, Zhu T, et al. Characterization of fibrinogen-like protein 2 (FGL2): Monomeric FGL2 has enhanced immunosuppressive activity in comparison to oligomeric FGL2. *Int J Biochem Cell Biol*. 2013;45(2):408–418.
47. Foerster K, Helmy A, Zhu Y, et al. The novel immunoregulatory molecule FGL2: A potential biomarker for severity of chronic hepatitis C virus infection. *J Hepatol*. 2010;53(4):608–615.
48. Ning Q, Lakatoo S, Liu M, et al. Induction of prothrombinase fgl2 by the nucleocapsid protein of virulent mouse hepatitis virus is dependent on host hepatic nuclear factor-4 alpha. *J Biol Chem*. 2003;278(18): 15541–15549.
49. Liu M, Mendicino M, Ning Q, et al. Cytokine-induced hepatic apoptosis is dependent on FGL2/fibroleukin: The role of Sp1/Sp3 and STAT1/PU.1 composite cis elements. *J Immunol*. 2006;176(11):7028–7038.
50. Han M, Yan W, Guo W, et al. Hepatitis B virus-induced hFGL2 transcription is dependent on c-Ets-2 and MAPK signal pathway. *J Biol Chem*. 2008;283(47): 32715–32729.